IOPscience iopscience.iop.org

Home Search Collections Journals About Contact us My IOPscience

Growth of gallium nitride by HVPE

This article has been downloaded from IOPscience. Please scroll down to see the full text article.

2001 J. Phys.: Condens. Matter 13 6893

(http://iopscience.iop.org/0953-8984/13/32/302)

View the table of contents for this issue, or go to the journal homepage for more

Download details:
IP Address: 171.66.16.226
The article was downloaded on 16/05/2010 at 14:04

Please note that terms and conditions apply.

INSTITUTE OF PHYSICS PUBLISHING JOURNAL OF PHYSICS: CONDENSED MATTER

J. Phys.: Condens. Matter **13** (2001) 6893–6905 PII: S0953-8984(01)24775-4

Growth of gallium nitride by HVPE

Robert Cadoret and Agnès Trassoudaine

LASMEA, UMR 6602 CNRS, Université Blaise Pascal de Clermont Ferrand, Les Cézeaux, 63177 Aubière cedex, France

Received 11 May 2001
Published 26 July 2001
Online at stacks.iop.org/JPhysCM/13/6893

Abstract

The two mechanisms involved in the growth of (00.1) GaN HVPE have been deduced from the numerous experiments performed on (001) GaAs by the chloride method. They include a desorption of adsorbed Cl as HCl by H_2 for the first mechanism and a desorption of two Cl as $GaCl_3$ by GaCl for the second one. Theoretical curves have been computed by taking into account the interactions between the mass transfer, approximated by a simple model, the parasitic GaN deposition and the kinetics. They give a good approximation to the expected and observed growth rate values. A new domain of growth experimentally observed in conditions of expected fast etching by HCl ensures growth rates of 50–60 μm h^{-1} without parasitic GaN deposit by using a suitable temperature profile. This profile is computed by considering a combined mechanism of Cl desorption by GaCl as $GaCl_2$ and of etching by HCl. The produced $GaCl_2$ has to be supposed to be decomposed fast with respect to the mass transfer velocity. Its formation rate in the vapour phase has to be supposed to be very slow with respect to the reverse reaction. These assumptions are in agreement with the difficulty of observing this species and the well known doubt of its existence.

1. Introduction

HVPE has played an important historical role in that it was the first [1] and, until the early eighties, the only method for growing epitaxial layers of gallium nitride [2–8]. The advantage of this technique was to grow thick buffer layers at high growth rates on available substrates. So, when in the nineties the GaN applications appeared interesting to be developed, HVPE came back [9–12] for its ability to grow thick GaN films without too many defects at relatively low cost. Hexagonal GaN thick layers have been widely obtained on sapphire substrates and cubic GaN has been grown on (001) GaAs [13–15]. The best quality of the epilayers has been achieved by coalescence of selectively grown GaN on patterned SiO_2 masks [16–19]. Free standing GaN substrates have been prepared for the first time by Kim *et al* [20] and Melnik *et al* [21]. In spite of the thermodynamic and mass spectrometry analysis [3, 4, 22, 23] and of the fluid dynamic studies [24, 25] performed, the intricate processes involved in this growth technique were not well understood. Our first objective has been to improve this understanding

 © 2001 IOP Publishing Ltd Printed in the UK

experimentally and by modelling. The results we obtained are developed in this paper. The high values of the growth rate with respect to the values observed when the growth process is only limited by the mass transfer, such as MOCVD, is to be related to an effect of the kinetics. When kinetics values are more than 10 μm h^{-1} the effect of mass transfer increases with the kinetics values. When low growth rate values are observed, as in InN [26–29], this does not necessarily mean a mass transfer limited process as in MOCVD. It can come from the thermodynamics of the system. The complexity of the physics involved explains the large variation of growth rates observed by changing the experimental parameters and the reactor geometry. The understanding of these systems first requires systematic experimental studies then their modelling. This has been done with the {001} GaAs epitaxy by the chloride method and the (00.1) GaN HVPE. As these two systems give a complementary and coherent understanding of the involved physics we will focus this paper on the physics deduced from the modelling. In the next part we present the relations between the epitaxy of {001} GaAs and (00.1) GaN then the two growth mechanisms involved in these two processes. The effects of mass transfer and parasitic GaN deposition are presented and discussed in the third part. The experimental results we obtained in expected conditions of fast etching by HCl are presented in the fourth part with their modelling, preceding a discussion and the conclusion.

2. Relations between the {001} GaAs and (00.1) GaN epitaxy

The growth rates of III–V compounds deposited by HVPE or the chloride methods generally present an increasing then a decreasing part with decreasing substrate temperature. Shaw [30–32] was the first scientist to measure systematically the growth rate of GaAs on {001}, $\{111\}_A$, $\{111\}_B$ and {110} substrates, with hydrogen as carrier gas and by using the chloride method, as a function of temperature and, for {001} substrates, as a function of the GaCl partial pressure. He was the first to show that a Langmuir GaCl adsorption isotherm could explain the decreasing part of the experimental curves with decreasing substrate temperature. Later we showed [33, 34] that a term of lateral interaction between GaCl adsorbed molecules had to be considered to explain the slight decrease of the GaAs growth rate observed at low temperature, by increasing the GaCl partial pressure. A first model assuming an adsorption of GaCl followed by a Cl desorption by hydrogen was elaborated to compute the growth rate. This desorption mechanism is labelled the H_2 mechanism. Surface diffusion was introduced and computed by fitting the experimental measures of Hollan *et al* [35–37] as a function of the substrate orientation, and of Gentner *et al* [38, 39] on 6° off {001} GaAs substrates, carried out at atmospheric and reduced pressures in hydrogen and helium. A second mechanism was evidenced by the possibility to grow in He by the chloride method, therefore without H_2. This mechanism appeared in H_2 at low temperature and high $AsCl_3$ molar fraction values. The GaCl surface coverage value computed in the H_2 mechanism was close to one just before the appearance of this second mechanism. A desorption mechanism of two adsorbed chlorine atoms by GaCl in $GaCl_3$ was therefore considered with an intermediate $GaCl_3$ adsorption step [40]. This mechanism is labelled the $GaCl_3$ mechanism.

The only experimental curves available for computing the model parameters in the GaN HVPE system were the (00.1) curves reported by Seifert *et al* [8]. In hydrogen as well as in helium the decreasing part of the growth rate as a function of the reverse temperature was also observed. Furthermore the coaxial arrangement of the gas inlet tubes and the orientation of the substrate with respect to the flow, prevented from extraneous deposition on the quartz walls before the substrate. The measured growth rates reached very high values with respect to the highest values reported in recent years, 800 μm h^{-1} against 100–120 μm h^{-1} [41, 42]. This large value difference indicates an important effect of the mass transfer and of the parasitic

GaN deposition, always observed on the quartz walls in most of the reactors. Therefore most of the results published in the last ten years could not be used to understand and model the (00.1) GaN HVPE.

The {001} GaAs model has therefore been applied to the (00.1) GaN HVPE. Its parameters have been deduced from the two experimental curves of Seifert *et al* [8]. With respect to the GaAs model we have added an intermediate HCl adsorption step as suggested by the quantum chemical study of Seifert *et al* [43]. The GaN adsorption surface coverage has no longer been overlooked. Furthermore an adsorption of NH_3 with an adsorption energy value of -24.8 kcal mol^{-1} has been considered. Such an adsorption was reported to occur in MOCVD [44], but the experimental data were not clearly reported as a function of the NH_3 partial pressure. We have therefore considered an NH_3 adsorption energy value which could be in agreement with the MOCVD results without being competitive in the HVPE process.

3. Growth mechanisms

The surface process of the model involves therefore the adsorption of NH_3 molecules, the adsorption of N atoms resulting from NH_3 decomposition, then the adsorption of GaCl molecules over the N atoms and finally the chlorine desorption.

Two desorption mechanisms of chlorine are considered, desorption in HCl_g molecules following a surface reaction with H_{2g} leading to an intermediate HCl adsorption state, and desorption in $GaCl_{3g}$ molecules following an absorption of GaCl on two GaCl underlying molecules, according to the reactions

$$2NGaCl + H_{2g} \Leftrightarrow 2NGa\text{–}ClH \quad (1)$$

$$NGa\text{–}ClH \Leftrightarrow NGa + HCl_g \quad (2)$$

$$2NGaCl + GaCl_g \Leftrightarrow 2NGa\text{–}GaCl_3 \quad (3)$$

$$2NGa\text{–}GaCl_3 \Leftrightarrow 2NGa + GaCl_{3g} \quad (4)$$

where g subscript is used for gas phase species.

The surface adsorption state is approached by applying the Bragg–Williams approximation to a one-monolayer model of adsorption on a (00.1) Ga plane. The surface coverage θ_v of the Ga plane, labelled as V, free for the NH_3 adsorption, is then expressed

$$\theta_v = 1 - \sum_{i \neq v} \theta_i = 1 - \theta_{NH_3} - \theta_N - \theta_{NGaCl} - \theta_{HCl} - \theta_{GaCl_3} - \theta_{NGa} \quad (5)$$

where the admolecules NGa–ClH and 2NGa–$GaCl_3$ are denoted HCl and $GaCl_3$. θ_i is the surface coverage of the molecule i.

The two overall reactions corresponding to the two growth mechanisms are

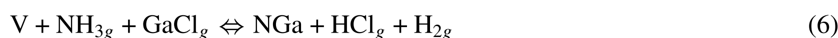
$$V + NH_{3g} + GaCl_g \Leftrightarrow NGa + HCl_g + H_{2g} \quad (6)$$

$$2V + 2NH_{3g} + 3GaCl_g \Leftrightarrow 2NGa + GaCl_{3g} + 3H_{2g}. \quad (7)$$

The $GaCl_3$ formation reaction in the gas phase is

$$GaCl_g + 2HCl_g \Leftrightarrow GaCl_{3g} + H_{2g}. \quad (8)$$

The θ_v surface coverage is computed by considering the surface–vapour equilibrium at a distance of the steps much larger than the diffusion mean free paths of adsorbed molecules. The growth rate is the product of the surface diffusion term by the maximal velocity, V_{Gmax}, reached for a distance between steps much lower than the double of the diffusion mean free

paths. The V_{GMax} expressions in the H_2 and $GaCl_3$ mechanisms are expressed

$$V_{GMaxH_2} = \frac{0.933\,57\theta_v}{N_s\sqrt{2\pi m_{HCl}kT}} P_{HCl}\gamma\alpha_{HCl}\exp\left(-\frac{\varepsilon_{HCl}+\Delta\varepsilon}{kT}\right) \tag{9}$$

$$V_{GMaxGaCl_3} = 2\frac{0.933\,57\theta_v}{N_s\sqrt{2\pi m_{GaCl_3}}} P^e_{GaCl_3}\left[(1+\gamma)^2 - \frac{P_{GaCl_3}}{P^e_{GaCl_3}}\right]\alpha_{GaCl_3}\exp\left(-\frac{\varepsilon_{GaCl_3}+2\Delta\varepsilon}{kT}\right). \tag{10}$$

The preexponential terms include the θ_v surface coverage, the P_i partial pressures, the relative supersaturation and the mass and the condensation coefficient of the HCl_g molecule in (9) and of the $GaCl_{3g}$ molecule in (10). k is the Boltzmann constant, N_s the number of GaN molecules per unit area. ε_i is the activation energy term. $P^e_{GaCl_3}$ is the homogeneous $GaCl_{3g}$ equilibrium partial pressure. $\Delta\varepsilon$ is the difference between the potential energies of a GaN molecule adsorbed on the surface and in a kink site. The following relations define the degree of excess of the deposition reaction in the H_2 and $GaCl_3$ mechanism:

$$\frac{P_{NH_3}P_{GaCl}}{P_{H_2}P_{HCl}K_6(T)} = 1+\gamma \tag{11}$$

$$\frac{P^2_{NH_3}P^3_{GaCl}}{P^3_{H_2}P_{GaCl_3}K_7(T)} = (1+\gamma)^2\frac{P^e_{GaCl_{3g}}}{P_{GaCl_3}} \tag{12}$$

with

$$P^e_{GaCl_{3g}} = \frac{P_{GaCl}P^2_{HCl}}{P_{H_2}K_8(T)}. \tag{13}$$

$K_i(T)$ is the equilibrium constant of the R_i reaction.

The relative supersaturation is defined as the degree of excess minus one. Its value is positive in conditions of growth, equal to zero at vapour–crystal thermodynamic equilibrium and negative in conditions of etching. Most of the GaN epitaxy experiments are carried out at high relative supersaturation values, which explains the usual parasitic deposition observed on the quartz walls. Therefore one of our first experimental objectives [45, 46] has been to research the conditions of vapour-crystal equilibrium by adding HCl to the main flow in N_2, H_2 and mixed N_2/H_2 gas carriers.

In the theoretical paper we published to describe the model [47] the $GaCl_3$ partial pressure was supposed to be in homogeneous equilibrium and the theoretical curves were computed by overlooking the $GaCl_3$ partial pressure value. Now the yield of $GaCl_3$ formation can be introduced in the software and the species balance equations take into account the $GaCl_3$g concentration.

The surface diffusion of NGa, NGaCl, NGaClH and $NGaCl_3$ molecules is to be considered. To simplify this intricate problem separate surface diffusion equations have been considered for NGa and NGaCl molecules [47]. The NGaCl resident time has been supposed to be determined by the evaporation frequency of GaCl, in order to include the resident time of HCl or $GaCl_3$ molecules. The NGa resident time has been deduced from the frequency of chlorination of NGa by HCl in the H_2 mechanism and by $GaCl_3$ in the $GaCl_3$ mechanism. This approach gives a variation of the growth rate with the misorientation angle with respect to (00.1) similar to the variation measured by Hollan *et al* [35–37]. The only parameters are the diffusion activation energies of NGaCl and NGa molecules. In the H_2 mechanism Pimpinelli *et al* have solved the actual diffusion equations of the GaAs model that has not considered the HCl intermediate step [48].

As detailed in [47] the reactions of GaCl adsorption over adsorbed N atoms and two adsorbed GaCl molecules, and the reactions of HCl and $GaCl_3$ adsorption on adsorbed NGa

molecules, have been expressed with the classical form:

$$\alpha_i \frac{P_i}{\sqrt{2\pi m_i kT}} \exp\left(-\frac{\varepsilon_i}{kT}\right) \tag{14}$$

where α_i is the condensation coefficient and α_i the activation energy of adsorption.

This form assumes that the molecule to be adsorbed is located over a potential energy barrier of height ε_i with the same number of degrees of freedom as the gaseous molecule but the translation of degree of freedom located over the barrier. The surface sites where the molecule is to be adsorbed are supposed to have their energy and vibration states unchanged. The corresponding activated molecule may be more complex; the difference between its entropy and the entropy involved in (14) is only included in the condensation coefficient if the activation potential energy is known, which is not the case. In the relations (9) and (10) $\varepsilon_{ai} = \varepsilon_i - kT \log \alpha_i$ is then the apparent activation energy of chlorination of NGa molecules by HCl or $GaCl_3$ gaseous molecules. The only model parameters to be determined are then ε_{aH_2}, ε_{aGaCl_3}, $\Delta\varepsilon$ and the adsorption energies of GaCl, HCl and $GaCl_3$ molecules from the vapour. The adsorption energy, ε_{adi}, of an i molecule is defined as the difference between the potential energies of the adsorbed and vapour molecules. The vibration term per degree of freedom of adsorbed molecules have been considered as the same as the GaN one. The vibration degree of freedom of GaN has been deduced by fitting the equilibrium curves versus $1/T$ of the reaction (6), calculated with the thermodynamic data [49] and with the partition functions.

The parameter values computed by fitting the theoretical and the Seifert [8] curves are
$\varepsilon_{adHCl} = -63.54$ kcal mol^{-1}, $\varepsilon_{adGaCl} = -130.46 - 8.14\theta_{GaCl} - 9.768\theta_{GaCl_3}$ kcal mol^{-1}
$\varepsilon_{adGaCl_3} = -71.49 - 9.768\theta_{GaCl}$ kcal mol^{-1}, $\Delta\varepsilon = 8.737$ kcal mol^{-1}
$\varepsilon_{aHCl} = 11.32 - 1.98572T \log(64.7 \exp(1.01 \times 10^{-2}(1223 - T)))$ kcal mol^{-1}
$\varepsilon_{aGaCl_3} = 7.74 - 1.98572T \log(2.6 \times 10^4 \exp(6.5 \times 10^{-3}(1230 - T)))$ kcal mol^{-1}.

The differences between these values computed by taking into account the $GaCl_{3g}$ concentration and the values reported in [47] are small.

The activation potential energy of GaN and NGaCl surface diffusion, 39.7 kcal mol^{-1}, and the ledge energy of the critical 2D nucleus of the spiral growth, 51.3 kcal mol^{-1}, have not been changed with respect to the values published in [47].

4. Research on the mass transfer and parasitic nucleation effects

When the degrees of excess of the deposition reactions are high, the ratios between the relative supersaturations and the corresponding degrees of excess are very close to one. The kinetics are then proportional to the vacant surface site coverage, to the source species concentrations and to the reverse of the hydrogen concentration as deduced from (9)–(13). The equilibrium constants, the activation terms and the value of θ_v mainly govern the kinetic variations with the substrate temperature. The H_2 concentration in neutral gas transport systems mainly depends on the rates of NH_3 decomposition and of hydrogen produced by the GaN parasitic deposition before the substrate, and on the mass transfer. The mass transfer reduces the partial pressures of the source species and increases the partial pressures of the produced species. These two effects can induce an H_2 mechanism in a neutral gas carrier. The mass of GaN deposited before the substrate can reduce the degrees of excess up to a value close to one if high. The mass transfer effect detailed in [47] is approached by considering a diffusion layer thickness equal to the velocity gradient thickness of an established Poiseuille regime, providing that the substrate is parallel to the flow and that the total flow is not too low. When the substrate makes an angle with respect to the horizontal plane, the mass transfer effect can be approached by varying the wall–substrate distance. Such an approach does not replace the fluid dynamic study for

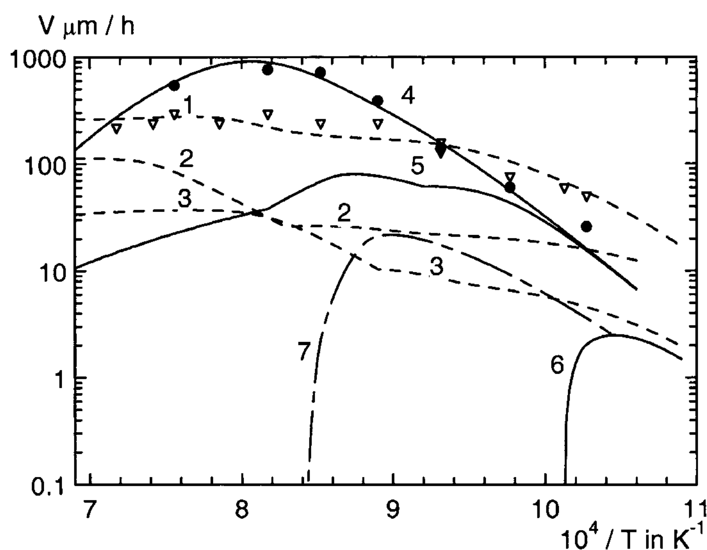

Figure 1. Experimental growth rates in μm h^{-1} measured by Seifert *et al* [8] in H_2 and He as carrier gas, on substrates 3° misoriented from the (00.1) orientation, are represented by full circles and empty triangles. The kinetics and the growth rates computed with the mass transfer and wall–substrate distances of 1.5 cm, without and with a parasitic GaN deposition of 2 g h^{-1} are drawn as dashed curves 1, 2 and 3 in He and as full curves 4, 5 and 6 in H_2. The dashed-dotted curve 7 shows the $GaCl_2$–HCl mechanism in the conditions of curve 6.

optimizing the working conditions of a reactor. On the other hand a fluid dynamic study is unable to determine the growth law, which is the boundary conditions to be known to solve the fluid dynamic equations.

The mass transfer and parasitic deposition effects are illustrated in figures 1 and 2. The experimental points measured by Seifert *et al* [8] in He and H_2 atmospheres are reported as empty triangles and full circles in figure 1. The dashed curves 1, 2 and 3 represent, in He, the theoretical kinetic results, the curve computed by assuming a mass transfer corresponding to a substrate–wall distance of 1.5 cm and the curve computed by adding a GaN parasitic deposition of 2 g h^{-1} to this mass transfer. The full curves 4, 5 and 6 represent the same theoretical results computed with H_2 as gas carrier. In H_2 atmosphere the growth rate increases slightly with $1/T$ up to about 1220 K. At lower temperatures the kinetic slope arising from the surface saturation by HCl and GaCl adsorptions appears progressively. The mass transfer effect reduces the growth rate of about an order of magnitude for kinetic values higher than 100 μm h^{-1}. The adding GaN parasitic deposition cancels the γ supersaturation at 988 K. Above this temperature value the GaN etching by HCl vapour molecules is expected, but the experiments we carried out [50, 51] showed that growth rates up to 50 μm h^{-1} could be obtained in the HCl etching field. The mechanism involved in this field is developed in the next section. The dashed–dotted curve 7 draws the corresponding theoretical results. In He atmosphere the growth rate variation with temperature is lower than in H_2. This comes from the fact that the $GaCl_3$ mechanism requires a high GaCl surface coverage. By decreasing temperature the $GaCl_3$ adsorption replaces progressively the GaCl one without changing drastically the θ_V value. The H_2 vapour concentration enhancement resulting from the mass transfer effect induces the H_2 mechanism at temperatures higher than 1210 K. This transition point between the H_2 and $GaCl_3$ mechanisms is shifted from 1210 K to 1120 K by adding a GaN parasitic deposition rate of 2 g h^{-1}.

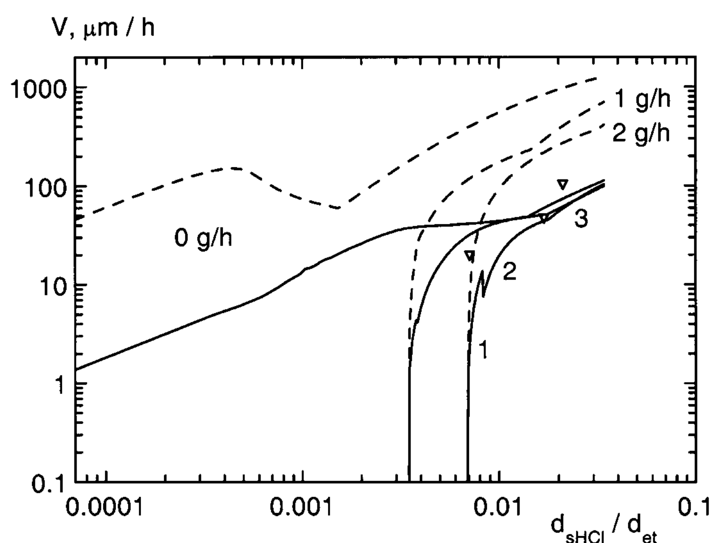

Figure 2. Theoretical kinetics and growth rates taking into account the mass transfer and wall-substrate distances of 1.5 cm are drawn as dashed and full lines, by considering no and parasitic GaN deposition of 1 and 2 g h^{-1} before the substrate, as a function of the source HCl concentration input. Parts 1, 2 and 3 correspond to the $GaCl_2$–HCl, H_2 and $GaCl_3$ prevailing mechanisms. The experimental conditions of Paskova *et al* [43], empty triangles, have been used.

The kinetic theoretical curves obtained in the experimental conditions of Paskova *et al* [52] without and with parasitic deposition rates of 1 g h^{-1} and 2 g h^{-1} are drawn as dashed lines in figure 2, as a function of the ratio of the Ga source HCl flow to the total flow. The H_2 mechanism prevailing field which appears only at values of this ratio lower than 0.0015 is extended up to to 0.015 then up to a value higher than 0.034 by adding a parasitic deposition rate of 1 g h^{-1} and 2 g h^{-1}. The corresponding curves drawn by considering a substrate–wall distance of 1.5 cm for the mass transfer are drawn as full lines. The H_2 mechanism prevails over a value of 0.015 of the source HCl vapour concentration input. At 0.0034 and 0.0068 values the effect of the GaN parasitic deposition cancels the relative supersaturation. By increasing the source HCl concentration input beyond this point the growth rate increases drastically, becoming almost constant. Parts 1, 2 and 3 of the 2 g h^{-1} full curve correspond to the mechanism developed in the next section and to the H_2 and $GaCl_3$ mechanisms. The three experimental points are reported as small triangles. The first point is located in a domain where the growth rate is very sensitive to the GaN parasitic deposition rate and to the source HCl concentration input. The second point is located in a domain where the growth rate is practically independent of these experimental parameters, which is in agreement with the constant value observed by the authors for different experiment times. The last point is the only one which seems to correspond to the $GaCl_3$ mechanism. The drastic change of the experimental slope can be related to the H_2–$GaCl_3$ mechanism transition.

5. New mechanism of growth at γ negative values

5.1. Experimental results

The experimental research of the zero supersaturation point with H_2 and N_2 as gas carriers has led us to find an unexpected new mechanism in a mixed N_2/H_2 gas carrier. The source, central

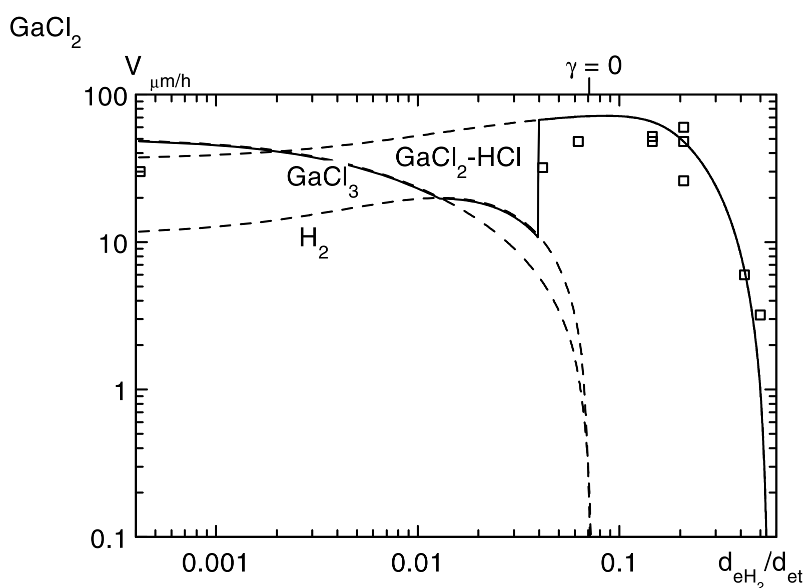

Figure 3. In the experimental conditions reported in section 5 the measured growth rates are represented by empty squares, as a function of the H_2 concentration input. The theoretical results are drawn as dashed curves for the H_2, $GaCl_3$ and $GaCl_2$–HCl mechanisms. The prevailing mechanism, $GaCl_3$, H_2 then $GaCl_2$–HCl is drawn as a full curve. The mass transfer is taken into account with wall–substrate distances of 1.5 cm.

and substrate zones were kept at 1123, 1293–1313 and 1253 K. In pure H_2 or N_2 systems the zero growth rate point was obtained by adding HCl in the main flow, with a reasonable accuracy, at the vapour-crystal equilibrium [50, 51]. In N_2 the results suggested that the $GaCl_3$ vapour concentration was below but not too far from its homogeneous equilibrium value, that was around 10^{-3} atmosphere. The large amount of HCl added in the main flow, 200 sccm, explains this high value. A parasitic GaN deposition was obtained even without growth on GaN substrates, which probably comes from the times required for reaching the homogeneous equilibrium $GaCl_3$ vapour concentration. In H_2 this problem was not encountered but if the reduction of the relative supersaturation decreases effectively the parasitic GaN deposition it also reduces the growth rate. Below a degree of excess of about 4 no growth occurs on sapphire substrates.

In a range of N_2/H_2 mixing varying with the experimental conditions, the growth rate did not depend on the added HCl flow and values of 50–60 μm h^{-1} could be obtained with very negative values of the γ supersaturation, then in expected conditions of fast etching by HCl. A first set of experiments were performed with 2000 sccm of N_2, 300 sccm of NH_3 and 20 sccm of HCl mixed with 83 sccm of nitrogen on the gallium source and without additional HCl. The hydrogen added in the main flow was varied from 0 to 2000 sccm, the total amount of the gas carrier flow staying at a constant value of 2000 sccm. In the 0–650 sccm H_2 flow range growth and extraneous deposit upstream of the substrate were observed. For 800, 1000 and 2000 sccm of H_2 flows no growth parasitic deposit occurs. The experiments showed that the nucleation critical relative supersaturation value of GaN was close to 4 on sapphire substrate and higher than this value on quartz. Therefore there is a small domain of relative supersaturation values available to get the highest possible growth rate with a reduced GaN parasitic deposition. This domain seems not to exist with pure N_2 as gas carrier.

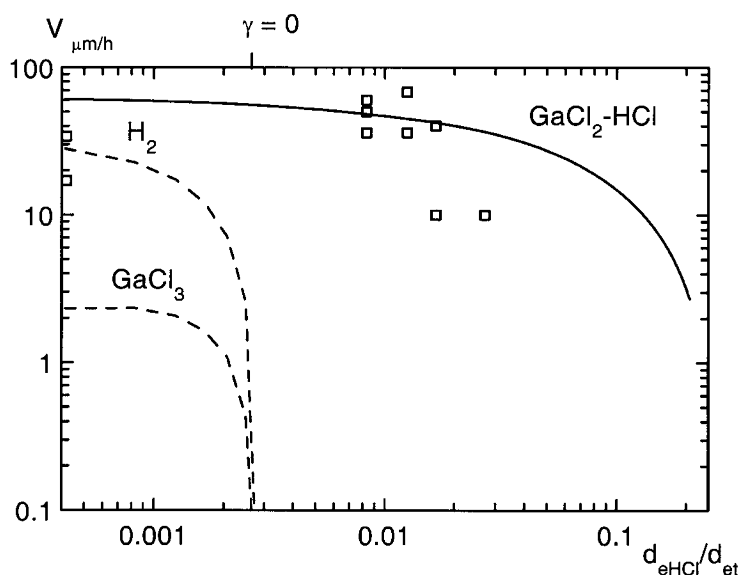

Figure 4. In the experimental conditions reported in section 5 the measured growth rates are represented by empty squares, as a function of the additional HCl concentration input. The theoretical results are drawn as dashed curves for the $GaCl_3$ and H_2 mechanisms. The prevailing mechanism drawn in full curve is $GaCl_2$–HCl. The mass transfer is taken into account with wall–substrate distances of 1.5 cm.

A second set of experiments was performed with the same total and NH_3 flows, HCl and N_2 flows on the gallium source, and with 20 sccm of additional HCl. The hydrogen added in the main flow was varied from 0 sccm to 1200 sccm. The parasitic deposit observed in the mixing zone decreased with increasing the flow of hydrogen, and finally almost disappeared for 500 sccm of hydrogen. The experimental points are reported and the growth rates, computed in the H_2 and $GaCl_3$ mechanisms, are drawn as dashed lines in figure 3. The third theoretical mechanism, labelled $GaCl_2$–HCl, is also drawn as a dashed line. The prevailing mechanism is drawn as a full line. The mass transfer was calculated with a substrate–wall distance of 1.5 cm. By increasing the H_2 flow the theoretical curves show that the prevailing mechanism is $GaCl_3$ up to 30 sccm, then H_2 up to 96 sccm and the third mechanism up to 1330 sccm, with the total flow of 2403 sccm. The zero point of the γ relative supersaturation occurs with an H_2 flow value of 175 sccm, at the drop of the H_2 and $GaCl_3$ curves. At a H_2 flow of 500 sccm, $\gamma = -0.63$, the experimental growth rate reached a value of 60 μm h^{-1}. Above 500 sccm the growth rate measured on GaN substrates drastically drops. Its zero value is reached at 1330 sccm of H_2.

A third set of experiments was performed at 500 sccm of H_2 with additional HCl flow values of 20, 30, 40, 60 and 65 sccm. The experimental points are reported and the growth rates computed in the H_2 and $GaCl_3$ mechanisms are drawn as dashed lines in figure 4. At 40 sccm the growth rate value is 40 μm h^{-1} on GaN and 10 μm h^{-1} on sapphire substrates. At 65 sccm the 10 μm h^{-1} value was measured on a GaN substrate. The zero γ value corresponds to an additional HCl flow of 6.5 sccm. For 20, 30, 40 and 65 sccm the γ values are -0.63, -0.75, -0.81 and -0.89. The theoretical $GaCl_2$–HCl mechanism is drawn as a full line.

5.2. Third growth mechanism

The first computations made by using the software, without changing its parameter, reveals that the drop of the growth rate at 1330 sccm of H_2 comes from the etching by HCl. A new dechlorination mechanism was to be considered and therefore its reverse reaction was also to be taken into account. The criterion to select between the etching of NGa by the reverse reaction of the new dechlorination mechanism and by HCl had to be the ratio between these two etching fluxes. For values lower than one the combined mechanism with etching by HCl had to be considered.

The theoretical curve matching the experimental points reported in Figure 3 at negative γ values was obtained by considering a dechlorination of NGaCl by $GaCl_g$ in $GaCl_{2g}$ and a chlorination of NGa by HCl followed by H2g desorption for the reverse reaction. The involved reactions are

$$\mathrm{NaGaCl} + \mathrm{GaCl}_g \Rightarrow \mathrm{NGa} + \mathrm{GaCl}_{2g} \quad (15)$$

$$\mathrm{NGa} - \mathrm{HCl} \Leftarrow \mathrm{NGa} + \mathrm{HCl}_g \quad (16)$$

$$2\mathrm{NGaCl} + \mathrm{H}_{2g} \Leftarrow 2\mathrm{NGa} - \mathrm{HCl} \quad (17)$$

$$\mathrm{NGaCl} + \mathrm{GaCl}_g \Leftarrow \mathrm{NGa} + \mathrm{GaCl}_{2g} \quad (18)$$

and for the equilibrium vapour reaction

$$\mathrm{HCl}_g + \mathrm{GaCl}_g \Leftarrow \mathrm{GaCl}_{2g} + \tfrac{1}{2}\mathrm{H}_{2g}. \quad (19)$$

By assuming a simple adsorption process for reactions (15) and (16) the GaN growth flux is written

$$J_{GaN} = \frac{P_{GaCl}}{\sqrt{2\pi m_{GaCl} kT}} \exp\left(-\frac{\varepsilon_{aGaCl}}{kT}\right)\frac{\theta_{NGaCl}}{N_s} - \frac{P_{HCl}}{\sqrt{2\pi m_{HCl} kT}} \exp\left(-\frac{\varepsilon_{aHCl}}{kT}\right)\frac{\theta_{NGa}}{N_s}. \quad (20)$$

The curves drawn in figures 3 and 4 for this combined mechanism, labelled $GaCl_2$–HCl, were computed with an apparent activation energy of the dechlorination reaction by GaCl into $GaCl_{2g}$, exceeding by only 1.49 kcal mol^{-1} the activation energy of the etching reaction by HCl. This adding parameter was the only modification of the model parameters. The maximal velocity is given by the same relation (9) as in the H_2 mechanism with, in place of γ, a relative supersaturation γ_{mix} given by

$$1 + \gamma_{mix} = (1+\gamma)\sqrt{\frac{m_{HCl}}{m_{GaCl}}}\frac{P_{GaCl}}{\sqrt{kTP_{H_2}}}\frac{\sqrt{z_{H_{2g}}}}{z_{HCl_g}}\frac{z_{NGaCl}}{z_{NGa}}\exp\left(-\frac{1.49\times 10^3}{1.9857T}\right) \quad (21)$$

where z_i and z_{ig} are the partition functions of the adsorbed molecule i and of the vapour molecule ig in a unit volume.

6. Discussion

The relation (21) shows the variation of the growth rate with the H_2 and GaCl partial pressures. The variation with the H_2 partial pressure is governed by γ_{mix}, which cancels at 1330 sccm of H_2 flow in our experimental conditions. The variation with the HCl partial pressure mainly comes from $\gamma_{mix}/(1+\gamma)$. The variation with temperature from the partition functions is illustrated in figure 5, where the curves computed with the H_2, $GaCl_3$ and $GaCl_2$–HCl mechanisms are drawn as dashed lines as a function of $1/T$, with 500 sccm of H_2 and 20 sccm of additional HCl flow. The γ value is negative at $T > 1087$ K. The prevailing mechanism, drawn as a full line, is the H_2 one at $T < 1010$ K and the $GaCl_2$–HCl one over this value. The growth rate drastically

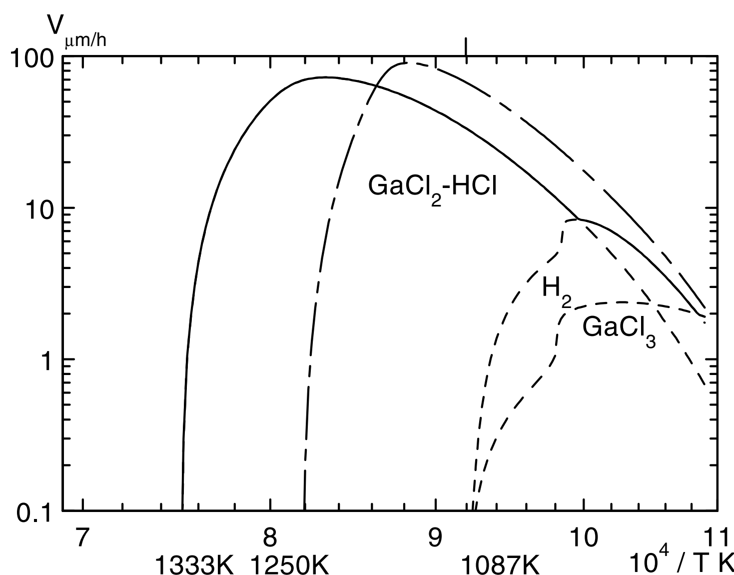

Figure 5. In the experimental conditions reported in section 5 the theoretical results are drawn in dashed curves for the $GaCl_3$, H_2 and $GaCl_2$–HCl mechanisms. The prevailing mechanism, $GaCl_2$–HCl then H_2 is drawn as a full curve. The dashed–dotted curve represents the theoretical results obtained with only H_2 in the main line; the only available mechanism is $GaCl_2$-HCl. The mass transfer is taken into account with wall–substrate distances of 1.5 cm.

drops at $T = 1333$ K at $\gamma_{mix} = 0$. The curve shows that a growth rate of 50–60 μm h^{-1} can be obtained without any parasitic GaN deposition with central and substrate temperature values of 1060 and 980 °C, in these experimental conditions. In our conditions where these values were 1020–1040 and 980 °C we observed only a very slight parasitic GaN deposition. With only hydrogen in the main line, 1980 sccm, the dashed–dotted curve of figure 5 represents the growth rate variation with the reverse temperature. The prevailing mechanism is $GaCl_2$–HCl. The relative supersaturation of this mechanism, γ_{mix} cancels at $T = 950$ °C, while the γ relative supersaturation is negative at $T = 654$ °C. The growth rate maximum of 90 μm h^{-1} is reached at 863 °C with a γ_{mix} value of about 25, which is too high to avoid parasitic GaN deposition. At 895–890 °C the growth rate value is about 50 μm h^{-1} and the range of γ_{mix} values, 4.1–5.6, ensures nucleation on sapphire and not on quartz. Therefore in hydrogen, a growth rate of 50 μm h^{-1} can be obtained without any parasitic GaN deposition with central and substrate temperature values of 950 and 895 °C. According to the theoretical curve 7 of figure 1 a growth rate of 20 μm h^{-1} could be obtained without parasitic GaN deposition with central and substrate zone temperatures of 915 and 855 °C.

The prevailing of the combined $GaCl_2$–HCl mechanism over the $GaCl_2$ one supposes that the ratio between the etching flux by HCl and by $GaCl_2$ is higher than one. According to the curve drawn as a full line in figure 3 as a function of the H_2 vapour concentration this occurs at 95 sccm of H_2 flow. This agreement with the experimental results can only be obtained by considering that the partial pressure of $GaCl_2$ is lowered to its heterogeneous or homogeneous equilibrium value, depending on whether the first or the second value is the smallest. Moreover the $GaCl_2$ partial pressure input has to be less than 10% of its homogeneous equilibrium value. That means (i) the $GaCl_2$ produced is rapidly transformed in HCl and GaCl, as supposed to compute the mass transfer, and (ii) the $GaCl_2$ homogeneous decomposition is much faster than its reverse reaction. This is in agreement with the fact that this species was

not observed by Ban [3]. Without these hypothesis the pure $GaCl_2$ mechanism would prevail at negative γ values up to about 300 sccm of H_2, in the experimental conditions of figure 3. The agreement with the experimental results could not be obtained. Indeed the mass transfer reduces the growth rate of the $GaCl_2$ mechanism to a small value even by assuming that the $GaCl_2$ partial pressure is lowered to its homogeneous equilibrium value. We used the GaCl diffusion coefficient in vapour to calculate this mass transfer, having no data on the $GaCl_2$ molecule. The $GaCl_2$ equilibrium pressures have been calculated with the thermodynamic data of Chatillon *et al* [53] which are in better agreement with the mass spectrometry analysis [3] than the thermodynamic data of Barin [54]. The last data lead to values about three orders of magnitude higher than the first data.

The theoretical curve of the $GaCl_2$–HCl mechanism, drawn as a function of the additional HCl concentration input seems to drop at higher values than observed. At high additional HCl flows the produced $GaCl_2$ may be not totally decomposed down to its heterogeneous equilibrium partial pressure. This hypothesis assumes that the decomposition rate is much higher than the mass transfer. A slight enhancement of the $GaCl_2$ partial pressure would lead to a drop of the curve at lower additional HCl flow than observed on the theoretical $GaCl_2$–HCl curve, by increasing the $GaCl_2$ etching over the HCl one.

7. Conclusion

The numerous measurements of the growth rate of exact and misoriented $\{001\}$ GaAs substrates by using the chloride method and the measures of Seifert *et al* [8] in He and H_2 on 3° off (00.1) GaN by HVPE, enabled us to model and understand the physics involved in the growth processes. The GaN kinetics being about one order of magnitude higher than the GaAs kinetics the mass transfer is larger for the first than the second system. Moreover the high supersaturation usually imposed leads to an important parasitic GaN deposition before the zone substrate that reduces and even can cancel the relative supersaturation. The method used to understand and model the GaAs and GaN growth processes can be applied to other IIIN compounds. The first requirements are to measure the growth rate in controlled conditions, and to study the thermodynamic of the system.

The modelling of the results obtained in expected conditions of fast HCl etching explains the physics involved in this process. It enables us to research, by computing, all the possibilities of growth at rates of 50–100 μm h^{-1} and more, without GaN parasitic deposition, by setting the central zone at higher and the substrate zone at lower temperatures so that the temperature of γ_{mix} cancels. It is quite a new possibility to explore experimentally and by computing the theoretical curves. In other systems the evidenced combined mechanism is also to be researched.

References

[1] Maruska H P and Tietjen J J 1969 *Appl. Phys. Lett.* **15** 327–9
[2] Wickenden D K, Faulkner K R and Brander R W 1971 *J. Cryst. Growth.* **9** 158–64
[3] Ban V S 1972 *J. Electrochem. Soc.* **119** 761–5
[4] Ilegems M 1972 *J. Cryst. Growth* **13/14** 360–4
[5] Shintani A and Minagawa S 1974 *J. Cryst. Growth* **22** 1–5
[6] Sano M and Aoki M 1976 *Japan. J. Appl. Phys.* **15** 1943–50
[7] Madar R, Michel D, Jacob G and Boulou M 1977 *J. Cryst. Growth* **40** 239–52
[8] Seifert W, Fitzl G and Butter E 1981 *J. Cryst. Growth* **52** 257–62
[9] Naniwae K, Itoh S, Amano H, Itoh K, Hiramatsu K and Akasaki I 1990 *J. Cryst. Growth* **99** 381–4
[10] Detchprohm T and Hiramatsu K 1992 *Appl. Phys. Lett.* **61** 2688–90

[11] Hiramatsu K, Detchprohm T and Akasaki I 1993 *Japan. J. Appl. Phys.* **32** 1528
[12] Molnar R J, Nichols K B, Maki P, Brown E R and Melngailis I 1995 *Mater. Res. Soc. Symp. Proc.* vol 378 (Pittsburgh, PA: Materials Research Society) 479
[13] Kimura A, Yamaguchi A A, Sakai A, Sunakawa H, Nido M and Usui A 1996 *Japan. J. Appl. Phys.* **35** L1480–2
[14] Yamaguchi A A, Manako T, Sakai A, Sunakawa H, Kimura A, Nido M and Usui A 1996 *Japan. J. Appl. Phys.* **35** L873–L875
[15] Tsuchiya H, Sunaba K, Suemasu T and Hasegawa F 1998 *J. Cryst. Growth* **189/190** 395–400
[16] Usui A, Sunakawa H, Sakai A and Yamaguchi A 1997 *Japan. J. Appl. Phys.* **36** L899–L902
[17] Hiramatsu K, Matsushima H, Shibata T, Sawaki N, Tadatomo K, Okagawa H, Ohuchi Y, Honda Y and Matsue T 1998 *Mater. Res. Soc. Symp. Proc.* vol 482 (Pittsburgh, PA: Materials Research Society) pp 257–68
[18] Shibata T, Sone H, Yahashi K, Yamaguchi M, Hiramatsu K, Sawaki N and Itoh N 1998 *J. Cryst. Growth.* **189/190** 67–71
[19] Nataf G, Beaumont B, Bouillé A, Haffouz S, Vaille M and Gibart P 1998 *J. Cryst. Growth* **192** 73–8
[20] Kim S T, Lee Y J, Moon D C, Hong C H and Yoo T K 1998 *J. Cryst. Growth* **194** 37–42
[21] Melnik Y, Nikolaev A, Nikitina I, Vassilevski K and Dimitriev V 1998 *Mater. Res. Soc. Symp. Proc.* vol 482 (Pittsburgh, PA: Materials Research Society) pp 269–74
[22] Ilegems M and Montgomery H C 1973 *J. Phys. Chem. Solid* **34** 885
[23] Koukitu A, Hama S, Taki T and Seki H 1998 *Japan. J. Appl. Phys.* **37** 762–5
[24] Karpov S Y, Zimina D V, Makarov Y N, Beaumont B, Nataf G, Gibart P, Heuken M, Jürgensen H and Krishnan A 1999 *Phys. Status Solidi* a **176** 439–42
[25] Meyyappan M 1997 *J. Vac. Sci. Technol.* A **16** 685–8
[26] Sato Y and Sato S 1994 *J. Cryst. Growth* **144** 15–19
[27] Sunakawa H, Yamaguchi A A, Kimura A and Usui A 1996 *Japan. J. Appl. Phys.* **35** L1395–7
[28] Takahashi N, Matsumoto R, Koukitu A and Seki M 1997 *Japan. J. Appl. Phys.* **36** L743–5
[29] Takahashi N, Ogasawara J and Koukitu A 1997 *J. Cryst. Growth* **172** 298–302
[30] Shaw D W 1968 *J. Electrochem. Soc.* **115** 405
[31] Shaw D W 1968 *J. Electrochem. Soc.* **115** 777
[32] Shaw D W 1970 *J. Electrochem. Soc.* **117** 683
[33] Cadoret R 1980 *Current Topics in Materials Science* vol 5, ed E Kaldis (Amsterdam: North-Holland)
[34] Theeten J B, Hollan L and Cadoret R 1977 *Crystal Growth and Materials* ed E Kaldis and H J Scheel (Amsterdam: North-Holland)
[35] Hollan L and Schiller C 1972 *J. Cryst. Growth* **13/14** 319
[36] Hollan L and Schiller C 1974 *J. Cryst. Growth* **32** 175
[37] Hollen L, Durand J M and Cadoret R 1977 *J. Electrochem. Soc.* **214** 135
[38] Gentner J L, Bernard C and Cadoret R 1982 *J. Cryst. growth* **56** 332
[39] Gentner J L and Cadoret R 1982 *J. Physique Coll.* **43** C5
[40] Cadoret R and Gil-Lafon E 1997 *J. Physique* I **7** 889–907
[41] Golan Y, Wu X H, Speck J S, Vaudo R P and Phanse V M 1998 *Appl. Phys. Lett.* **73** 3090
[42] Zhang R and Kuech T F 1998 *Mater. Res. Soc. Symp. Proc.* vol 482 (Pittsburgh, PA: Materials Research Society) p 709
[43] Seifert W, Swchatlick S, Reinhold J and Butter E 1984 *J. Cryst. Growth* **66** 333
[44] Briot O, Chur S and Aulombard 1997 *Appl. Phys. Lett.* **71** 1990
[45] Trassoudaine A, Aujol E, Disseix P, Castelluci D and Cadoret R 1999 *Phys. Status Solidi* a **176** 425–8
[46] Aujol E, Trassoudaine A, Castelluci D and Cadoret R 2001 *Mater. Sci. Eng.* B **82** 65–7
[47] Cadoret R 1999 *J. Cryst. Growth* **205** 123
[48] Gil-Lafon E, Napierala J, Pimpinelli A, Cadoret R and Trassoudaine A 2001 *J. Cryst. Growth* at press
[49] Aujol E, Napierala J, Trassoudaine A, Gil-Lafon E and Cadoret R 2001 *J. Cryst. Growth* **222** 538–48
[50] Aujol E, Trassoudaine A, Siozade L, Pimpinelli A and Cadoret R 2001 *J. Cryst. Growth* at press
[51] Trassoudaine A, Aujol E, Cadoret R, Paskova T and Monemar B 2000 *Mater. Res. Soc. Symp. Proc.* at press
[52] Paskova T, Svedberg E B, Madsen L D, Yakimova R, Ivanov I G, Henry A and Monemar B 1999 *MRS Internet J. Nitride Semicond. Res.* **4S1** G3.16
[53] Chatillon C and Bernard C 1985 *J. Cryst. Growth* **71** 433
[54] Barin I 1993 *Thermodynamical Data of Pure Substances* (Weinheim: VCH)